Physicochem. Probl. Miner. Process., 56(1), 2020, 43-53

http://www.journalssystem.com/ppmp

Physicochemical Problems of Mineral Processing

ISSN 1643-1049

Received July 14, 2019; reviewed; accepted September 29, 2019

Mechanism of the combined effects of air rate and froth depth on entrainment factor in copper flotation

Lei Wang, Yaowen Xing, Jun Wang

National Engineering Research Centre of Coal Preparation and Purification, China University of Mining and Technology, China

Corresponding author: lei.wang@cumt.edu.cn (Lei Wang)

Abstract: The effect of air rate and froth depth on the entrainment factor in flotation has been extensively studied, but further investigation on the underlying mechanism for their effect is still required. In this study, flotation tests were performed at different air rates and froth depths in a 3 dm^3 continuously operated cell using an artificial copper ore. The results showed that entrainment factor was affected by both air rate and froth depth, and the combined effect of these variables on entrainment factor depended strongly on the particle size. The entrainment factor increased with either increasing air rate at a relatively shallow froth or decreasing froth depth at a relatively high air rate. At a very low air rate and deep froth, higher entrainment factor was observed for mid-size and coarse particles. When the entrainment factor was correlated to the effective liquid velocity at the pulp/froth interface, the results indicated that multiple mechanisms were responsible for the effect on entrainment factor. At a relatively high air rate and shallow froth depth, entrainment factor had a linear relationship with the interface effective liquid velocity, suggesting that drag force dominated the change in the entrainment factor when air rate and froth depth were varied. At a very low air rate and deep froth, the entrainment factor for fine particles was found to correlate strongly with the interface effective liquid velocity, while the entrapment of solid particles may be the main reason for the high entrainment factor for mid-size and coarse particles under this condition.

Keywords: froth flotation, copper, entrainment, air rate, froth depth

1. Introduction

In froth flotation, entrainment is a principal mechanism responsible for the recovery of gangue material in the concentrate, which determines the grade of the final product. Entrainment is generally considered as a two-step process: particles first ascend from the region below the pulp/froth interface into the froth and then move from the froth into the concentrate (Zheng et al., 2006b). The entrainment recovery of a gangue mineral depends on its entrainment factor (i.e., the degree of entrainment) and the water recovered into the concentrate (Johnson, 1972). Entrainment factor is a measure of the degree to which particles settle with respect to the water in the froth and pulp, which represents the degree of classification due to the drainage of solids relative to water in the froth and incomplete solids suspension in the pulp (see Eq. 1) (Johnson, 1972; Zheng et al., 2005). It can be used not only to estimate the entrainment recovery of various gangue minerals in a flotation system but also to quantify the contributions of entrainment and true flotation to the overall recovery of a valuable mineral (Savassi et al, 1998). Given the important role of entrainment factor in flotation, over decades extensive studies have been carried out to identify its significant variables (Englebrecht and Woodburn, 1975; Cutting et al., 1981; Lynch et al., 1981; Smith and Warren, 1989; Maachar and Dobby, 1992; Nelson and Lelinski, 2000; Nguyen and Schulze, 2004; Zheng et al., 2006b; Neethling and Cilliers, 2009; Yianatos and Contreras, 2010; Wang et al., 2016a; Kracht et al., 2016), to understand the mechanisms associated with these variables (Szatkowski, 1987; Smith and Warren, 1989; Zheng et al., 2006b; Neethling and Cilliers,

DOI: 10.5277/ppmp19071

2009; Wang et al., 2017), and to develop models for entrainment prediction and process optimization (Bisshop and White, 1976; Ross and Van Deventer, 1988; Savassi et al., 1998; Zheng et al., 2005; Neethling and Cilliers, 2009; Yianatos and Contreras, 2010; Wang et al., 2016b).

$$ENT = \frac{(Mass\ of\ free\ gangue\ per\ unit\ mass\ of\ water)_{concentrate}}{(Mass\ of\ free\ gangue\ per\ unit\ mass\ of\ water)_{tailing}}, \tag{1}$$

where *ENT* is the entrainment factor. Note that the free gangue minerals used for Eq. 1 refer to those being fully-liberated and non-floatable. However, it is not always easy to obtain this type of information in a real ore system. This is because the gangue minerals in the feed are almost always locked to some degree with valuable minerals, especially in the coarse size fractions. This undoubtedly causes errors when the entrainment factor is calculated as a proportion of the gangue in the concentrate which has been recovered by flotation rather than just entrainment. Liberation data can potentially be used to overcome this problem but mineral liberation analysis suffers from stereological error which means that not all the ''liberated gangue minerals" are actually fully liberated. Ideally, entrainment studies should be performed using liberated gangue or added gangue tracers that are known to be fully liberated (Wang et al., 2016b).

In flotation, air rate and froth depth are often adjusted to achieve a desired flotation performance (Bisshop and White, 1976; Zheng et al., 2006b). It is generally thought that these two variables affect the froth residence time, which in turn affects the relative drainage of solids to water (Bisshop and White, 1976; Zheng et al., 2006b). However, experiments have shown that the entrainment factor is relatively independent of froth residence time (Szatkowski, 1987; Wang et al., 2016a). Moreover, the concentration of gangue solid particles observed at different heights within a froth was found to remain constant after an initial decrease at the pulp/froth interface (Szatkowski, 1987). These observations suggest that the classification of entrained solids occurs primarily at the pulp/froth interface, and that using froth residence time to interpret the effect of air rate and froth depth on the entrainment factor may be misleading.

Neethling and Cilliers (2002a,b) proposed that gangue solid motion in a froth is the result of liquid motion, particle settling, and particle dispersion. A recent study by Wang et al. (2017) investigated the effects of the frother on entrainment factor, and showed a correlation between the entrainment factor and the effective liquid velocity at the pulp/froth interface. This effective liquid velocity is the velocity of the net water flow across the interface, which is a result from the balance of water moving upwards and water drainage at that region (Neethling and Cilliers, 2009). Since the flow was found to be laminar at the interface, Eq. (2) gives the relation between the interface effective liquid velocity and drag force (Elger et al., 2013; Wang et al., 2017). When the effective liquid velocity at the interface increases, the magnitude of the drag force on the particles also increases, and more solids overcome the downward gravitational force and move into the froth with the water, increasing the entrainment factor. This provides a clue to the mechanism behind the effect of air rate and froth depth, since both variables can also affect the water flowing into a concentrate. In view of this, Wang (2017) performed batch entrainment tests using quartz and a frother only at different air rates (J_g of 0.6 cm/s and 1.0 cm/s) and froth depths (1 cm and 2 cm) and observed a linear relationship between entrainment factor and the interface effective liquid velocity. Doubts about this conclusion have raised because only four tests were performed and no data were obtained from the test operated at a J_g of 0.6 cm/s and a froth depth of 2 cm. In addition, the experimental data were reported on an un-sized basis only, which is thought to be insufficient to support such a conclusion (Eq. 2).

$$F_D = bv, \tag{2}$$

where F_D is the drag force (N), v is the freestream velocity measured relative to the object (m/s), and b is a constant that depends on both the properties of the fluid (i.e., fluid viscosity), and the dimensions of the object (Kg/s).

In this study, the flotation tests were performed at different air rates and froth depths in a 3 dm^3 mechanical flotation cell using an artificial ore consisting of pure chalcopyrite and quartz. This work is an extension to previous work (Wang, 2017), aiming to elucidate the mechanism of the combined effects of air rate and froth depth on entrainment factor.

2. Materials and methods

Flotation tests were performed in a 3 dm^3 transparent, bottom-driven, perspex flotation cell (length, 12.5 cm; width, 12 cm; height, 20 cm) with a movable concentrate lip. The cell was operated continuously at different air rates (J_g of 0.7, 1.0, and 1.3 cm/s) and froth depths (1.5, 2.5, and 3.5 cm) in a closed circuit with a 50 dm^3 conditioning mixer. Fig. 1 shows a schematic diagram of the experimental set-up, which was expected to more closely mimic industrial flotation behaviours.

The feed to the tests was an artificial ore produced by combining chalcopyrite (purity > 95%) and quartz (purity of 99.5%). Chalcopyrite and quartz were both purchased from Ye Stone Trading Company as bulk rock, and were then crushed and wet ground to obtain a particle size of P_{80} 80 µm. The feed solids concentration was 40 wt.%, with a feed copper grade of 1%. The feed slurry pH was adjusted to 9.0 using 10 wt% sodium hydroxide (purity ≥ 99.7%). Sodium Ethyl Xanthate (SEX) (purity of 90%) (30 g/Mg) and Methyl Isobutyl Carbinol (MIBC) (purity of 98%) (15 ppm) were used as a collector and a frother, respectively.

The cell was operated at an impeller speed of 1000 rpm. Chalcopyrite is known to float fast, therefore the residence time was set at 1.5 min. Prior to setting air rates and froth depths, three residence times were required for the system to reach a steady state, which was determined in preliminary tests where the pulp level and flow rates to and from the flotation cell were kept constant. After that, samples of tailings, concentrate, and feed were taken over a period of 10 sec, and then filtered, dried, weighed, sampled, sized, and assayed for quartz. Sizing analyses were performed by wet screening with a set of sieves ranging from 20 to 150 µm.

Flotation reproducibility was assessed by conducting four replicates using an impeller of 1000 rpm, an air rate of 9.0 dm^3/min and a froth depth of 2.5 cm in preliminary tests. The relative standard errors of quartz recovery, water recovery, and entrainment factor on an un-sized basis at the 95% confidence interval were 3.94%, 5.83%, and 4.86%, respectively. This degree of error of quartz and water recovery is considered acceptable and sufficiently low to enable the effect of air rate and froth depth on the entrainment parameters to be determined with statistical confidence.

During each test, the effective liquid velocity at the interface (v_l) was estimated using Eq. 3 (Neethling and Cilliers, 2009). The net superficial liquid velocity (Q_l/A_c) was approximated by dividing the water flow measured in the concentrate (Q_l) by the cross-sectional area of the cell (A_c). Liquid holdup (ε) at the interface was approximated by sampling at four different locations using a modified sampler based on a methodology by Yianatos et al. (2001) (see Fig. 2). The sampler consists of a cylindrical tube with two plungers (having O-rings) attached to a central rod. The two plungers were set 1 cm apart, considering both the interference between the sampler and bubble size, and possible fluctuation of the local pulp/froth interface (Wang et al., 2017).

$$v_l = \frac{Q_l}{A_c}\frac{1}{\varepsilon} \tag{3}$$

where v_l is the effective liquid velocity at the pulp/froth interface (cm/s), Q_l is the volumetric liquid flowrate into the froth and overflowing the lip (cm^3/s), A_c is the cross-sectional area of the flotation cell (cm^2), and ε is the liquid holdup at the pulp/froth interface (%).

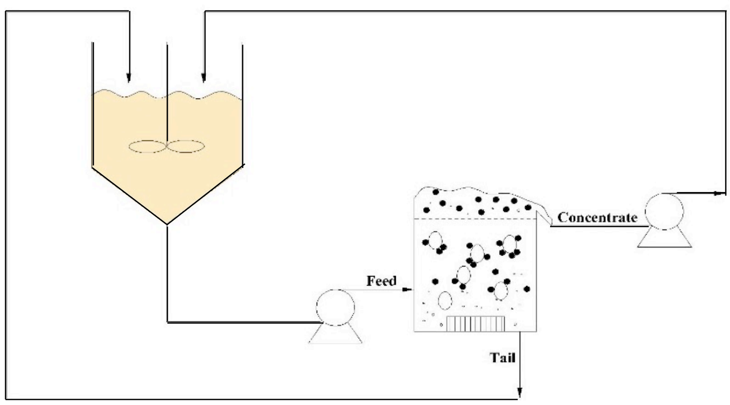

Fig. 1. Schematic diagram of the experimental set-up

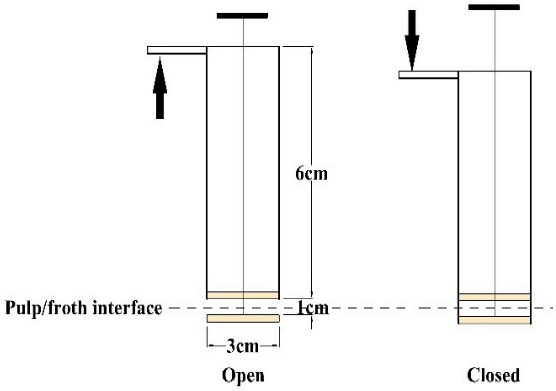

Fig. 2. Schematic diagram of the sampler used for liquid holdup measurements at the pulp/froth interface

3. Results and discussion

3.1. Entrainment test results

The quartz used in these tests was fully liberated and non-floatable, and will therefore be recovered into the concentrate only by entrainment (Wang et al., 2016a). A summary of the experimental results is presented in Table 1, which covers entrainment recovery of quartz (R_{quartz}), water recovery (R_{water}), and entrainment factor on an un-sized and size-by-size basis. Fig. 3 reveals that large variations in the quartz and water recovery occur when air rate and froth depth are varied. Note that the error bar (i.e.,standard deviation) in the figures of this study was estimated based on the four replicates in preliminary tests, unless stated otherwise. For a given air rate, both the recoveries decrease with increasing froth depth. When froth depth is kept constant, both the recoveries increase as air rate increases. The lowest values for quartz and water recovery are seen with an air rate of 6.3 dm^3/min and a froth depth of 3.5 cm, and the highest values are seen with an air rate of 11.7 dm^3/min and a froth depth of 1.5 cm. These trends agree with the results of other studies (Engelbrecht and Woodburn, 1975; Cutting et al., 1981; Langberg and Jameson, 1989; Zheng et al., 2006a; Wang et al., 2016c).

3.2. Effects of air rate and froth depth

Quartz recovery in different tests also changes as a consequence of variation in the entrainment factor, as presented in Table 1. Figs. 4 and 5 show the effect that air rate has on the entrainment factor for quartz on an un-sized and size-by-size basis, respectively. The entrainment factor changes noticeably when the air rate is varied. These changes not only depend on air rate but also on other flotation conditions such as froth depth and particle size. This suggests that air rate, froth depth and particle size interact to affect the entrainment factor in the flotation.

Table 1. Summary of the flotation test results at different air rates and froth depths

Air rate (dm^3/min)	6.3	6.3	6.3	9.0	9.0	9.0	11.7	11.7	11.7
Froth depth (cm)	1.5	2.5	3.5	1.5	2.5	3.5	1.5	2.5	3.5
R_{Quartz} (%)	6.20	1.69	0.69	12.01	4.55	1.44	17.71	8.14	2.74
R_{Water} (%)	18.23	7.42	3.01	29.38	14.38	7.78	35.12	22.02	12.09
$ENT_{unsized}$	0.297	0.214	0.223	0.328	0.284	0.173	0.398	0.314	0.205
$ENT_{+150\ \mu m}$	0.008	0.003	0.018	0.010	0.007	0.005	0.023	0.009	0.007
$ENT_{-150+106\ \mu m}$	0.016	0.004	0.022	0.017	0.012	0.005	0.038	0.016	0.006
$ENT_{-106+75\ \mu m}$	0.025	0.008	0.015	0.033	0.021	0.006	0.043	0.033	0.008
$ENT_{-75+53\ \mu m}$	0.041	0.029	0.028	0.050	0.026	0.012	0.086	0.047	0.017
$ENT_{-53+38\ \mu m}$	0.064	0.044	0.059	0.079	0.069	0.034	0.202	0.158	0.048
$ENT_{-38+20\ \mu m}$	0.178	0.142	0.098	0.244	0.185	0.113	0.352	0.225	0.179
$ENT_{-20\ \mu m}$	0.483	0.325	0.240	0.584	0.433	0.341	0.647	0.529	0.412

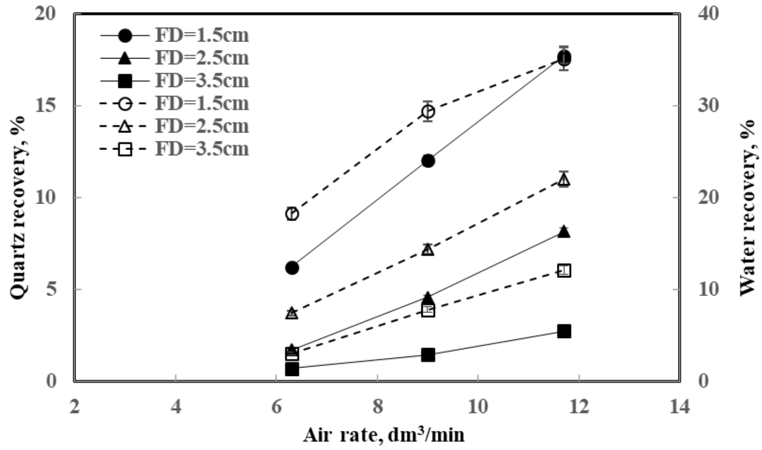

Fig. 3. Effect of air rate and froth depth on quartz recovery (solid line) and water recovery (dash line)

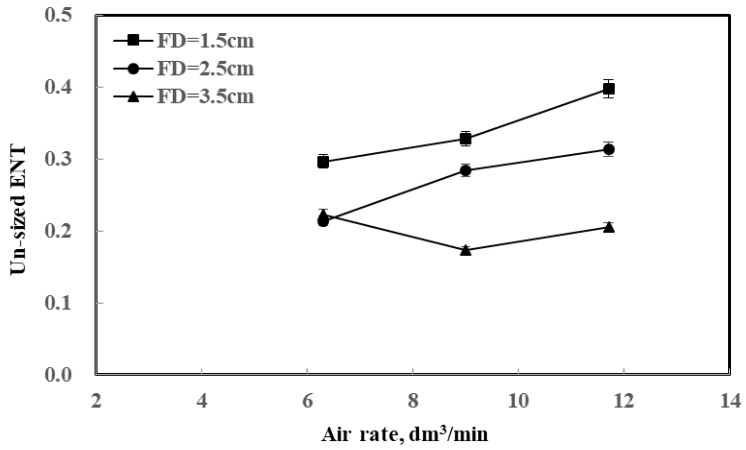

Fig. 4. Effect of air rate on the entrainment factor for quartz on an un-sized basis

In Fig. 4, the entrainment factor for quartz increases with the increasing air rate at froth depths of 1.5 cm and 2.5 cm. However, at a froth depth of 3.5 cm, the entrainment factor decreases first and then increases with the increasing air rate. Insight into these trends is gained by observing the effect of particle size shown in Fig. 5. For all size fractions, the entrainment factor increases with increasing air rate at froth depths of 1.5 cm and 2.5 cm. At a shallow froth, the entrainment factor for fine particles increases dramatically with increasing air rate. As particle size increases, this trend becomes less evident. Interestingly, at the froth depth of 3.5 cm, the entrainment factor for fine particles (below 38 μm) still increases with increasing air rate (see Fig. 5(a)), but for mid-size and coarse particles, the entrainment factor decreases first and then increases (see Fig. 5(b) and 5(c)).

Figs. 6 and 7 show the effect of froth depth on the entrainment factor for quartz on an un-sized and size-by-size basis, respectively. The entrainment factor varies with froth depth, and both air rate and particle size contribute to this effect. When the air rate is relatively high, the entrainment factor on an un-sized basis decreases with increasing froth depth. There is also a dramatic decrease in the entrainment factor for fine and mid-size particles as froth depth increases, but this trend is less evident for coarse particles. However, at an air rate of 6.3 dm^3/min, the entrainment factor on an un-sized basis fluctuates as froth depth increases. This is because on a size-by-size basis, the entrainment factor for coarse particles decreases first and then increases with increasing froth depth at an air rate of 6.3 dm^3/min.

3.3. ENT and effective liquid velocity at the interface

To understand the effect of air rate and froth depth on entrainment factor, the effective liquid velocity was estimated at the interface and correlated to the entrainment factor. Table 2 presents the superficial

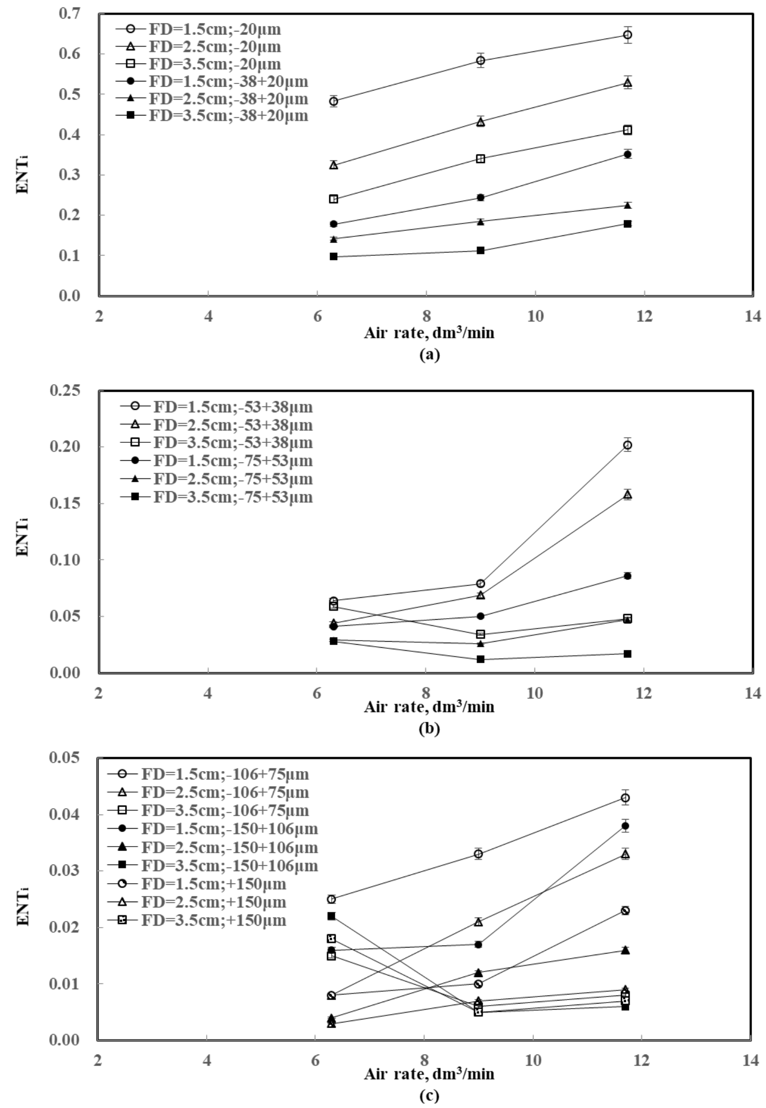

Fig. 5. Effect of air rate on the entrainment factor for quartz on a size-by-size basis

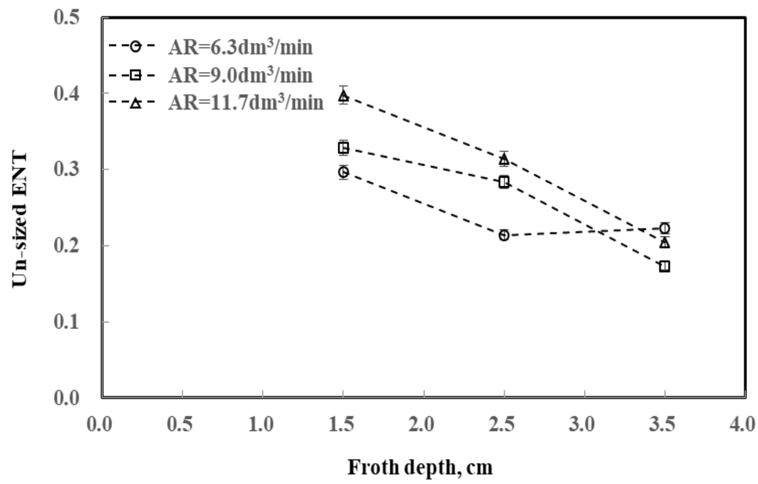

Fig. 6. Effect of froth depth on the entrainment factor for quartz on an un-sized basis

liquid velocity, interface liquid content, and interface effective liquid velocity obtained in different flotation tests. An increase in air rate or a decrease in froth depth leads to an increase in the superficial liquid velocity through the froth. Interestingly, the increasing either the air rate or froth depth increases the water content at the interface. Presumably, a deep froth exacerbates water drainage through the froth so that less water is recovered to the concentrate and more water remains at the interface. The increasing the air rate is more likely to result in bubble swarms that push more water across the interface into the froth (Smith and Warren, 1989), although this effect is counteracted to some extent because with a higher air rate, the froth residence time is shorter and there is less drainage of water from the upper froth.

As seen in Table 2, the effective liquid velocity at the interface varies greatly when either air rate or froth depth is varied. If the effective liquid velocity is the primary determinant of the effect of air rate and froth depth on the entrainment factor, there should be a single entrainment factor value that corresponds to one liquid velocity irrespective of air rate and froth depth. Fig. 8 shows the relationship between entrainment factor and effective liquid velocity at the interface. There was a positive linear correlation between entrainment factor and effective liquid velocity at the interface. The error bar represents the standard error at the 95% confidence intervals.

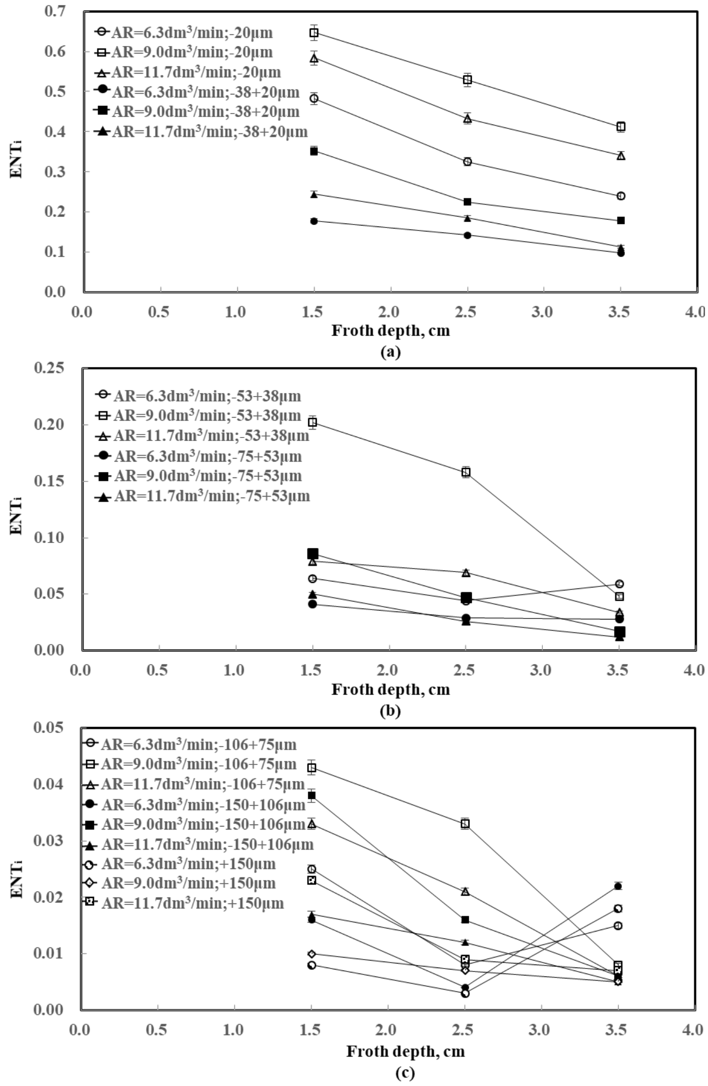

Fig. 7. Effect of froth depth on the entrainment factor for quartz on a size-by-size basis

Interestingly, the R^2 increases to 0.9058 from 0.8623 when removing the entrainment factor value (in red circle in Fig. 8) obtained at the lowest air rate (6.3 dm^3/min) and the deepest froth (3.5 cm). At a low air rate and deep froth, a low effective liquid velocity at the pulp/froth interface would be expected to result in a low entrainment factor. However, the high entrainment factor at a low air rate (6.3 dm^3/min) and a deep froth (3.5 cm) may imply that effective liquid velocity at the interface is not the only determinant of the entrainment factor, and other mechanisms may be involved. The high entrainment values seen on an un-sized basis are reproducible: the *ENT* values of four replicates re-conducted at the low air rate and deep froth were 0.221, 0.215, 0.229, and 0.217, which have a standard error of 0.0099 at the 95% confidence intervals.

Table 2. Effective liquid velocity at the pulp/froth interface in different flotation tests

Air rate (dm^3/min)	6.3	6.3	6.3	9.0	9.0	9.0	11.7	11.7	11.7
Froth depth (cm)	1.5	2.5	3.5	1.5	2.5	3.5	1.5	2.5	3.5
Q_l/A_c (cm/s)	0.0325	0.0134	0.0055	0.0521	0.0253	0.0135	0.0635	0.0389	0.0217
E (%)	62.12	63.78	65.85	69.26	71.05	73.21	75.41	70.69	80.17
V_l (cm/s)	0.0523	0.0210	0.0083	0.0753	0.0356	0.0185	0.0842	0.0550	0.0270

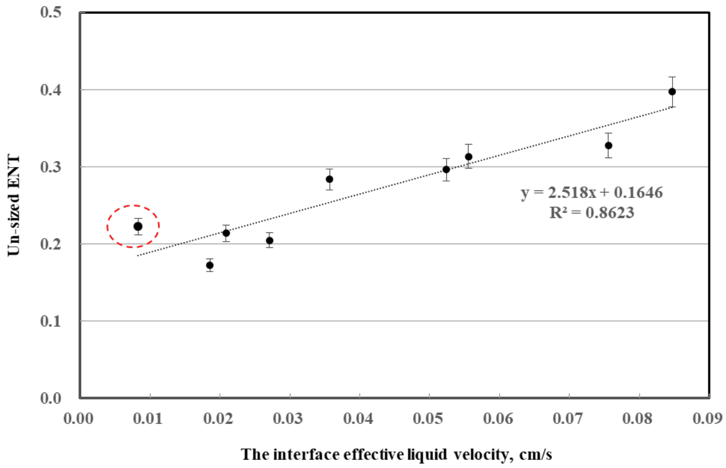

Fig. 8. Relationship between entrainment factor and effective liquid velocity at the interface on an un-sized basis

A high entrainment factor at a low air rate and deep froth was also observed in other flotation systems (Zheng et al., 2006b; Wang et al., 2016a). We speculate that entrapment mechanism accounts for this phenomenon. Entrapment typically occurs when the free settling of solid particles in the froth is retarded by narrowed plateau borders (see Fig. 9). Moreover, entrapment will become more apparent when valuable minerals are attached to the bubbles in the froth (Ata et al., 2004). A very low air rate and deep froth are expected to cause severe water drainage, resulting in a rapid narrowing of plateau borders in the froth (Ata et al., 2004; Zheng et al., 2006b). This reduces the drainage of mid-size and coarse particles, resulting in a high gangue concentration in the froth to which entrainment factor is proportional. An increase in the air rate with deep froth changes the structure of the froth, as evidenced by the sharp increase in the water content at the interface. This may lead to a water-rich channel that favors the drainage of mid-size and coarse particles from the froth. In addition, increasing the air rate also decreases the dynamic stability of the froth, which further promotes the drainage of particles, especially mid-size and coarse particles (Aktas et al., 2008). When the froth depth increases at a low air rate, it could severely hinder solid particles from settling in the plateau borders in the froth,

Fig. 9. Schematic diagram of solids entrapment in plateau borders at pulp/froth interface

which increases the entrainment factor. This entrapment mechanism explains the decrease in entrainment factor with increasing the air rate in deep froth, as shown in Figs. 4 and 5, and the increase in entrainment factor with the increasing the froth depth at the low air rate, as shown in Figs. 6 and 7.It is worth noting that, in the previous study (Wang et al, 2017), high entrainment factor did not occur when the effective liquid velocity at the interface was low. A number of ENT values fell below about 0.02 cm/s effective liquid velocity, but these all conformed to the linear prediction. This is probably because, at the low frother concentration of Dowfroth 250 and MIBC, a high rate of bubble coalescence and bursting within the froth tend to change the froth structure allowing an increased drainage of solids with respect to water, and solid particles cannot be easily entrapped (Ata et al., 2004; Wang et al., 2017). Since entrapment in flotation is generally difficult to distinguish from entrainment, the entrapment mechanism in this study still needs to be confirmed experimentally. Therefore, it is concluded that the effective liquid velocity at the interface dominates the entrainment factor when air rates and froth depths were varied, except for mid-size and coarse quartz particle (+38 μm) at a low air rate (6.3 dm^3/min) and a deep froth (3.5 cm). This correlation was investigated further by plotting these entrainment factor values against the effective liquid velocity at the interface on a size-by-size basis (Fig. 10). The entrainment factor increases linearly with increasing the effective liquid velocity at the interface. Moreover, the rate of entrainment factor increase decreases as particle size increases, as shown by the slopes of trendlines in Fig. 10. This suggests that the drag force caused by the upward movement of liquid at the interface and the gravitational force on the particles determine the motion of entrained solid particles in the flotation cell.

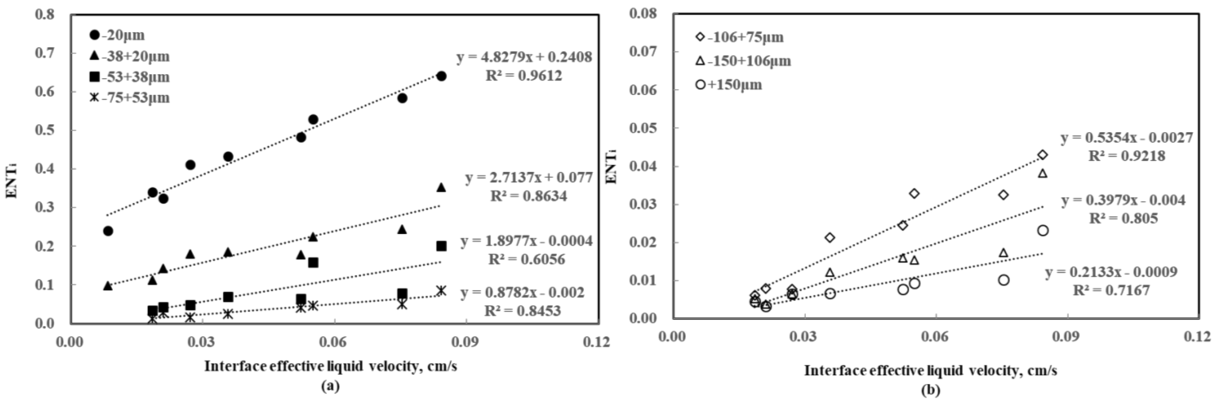

Fig. 10. Relationship between the effective liquid velocity at the interface and the entrainment factor for quartz particles on a size-by-size basis

In general, the increasing air rate or decreasing froth depth will result in a higher net liquid velocity through the plateau borders at the interface. This increases the drag force acting on the solid particles, resulting in a lower degree of solid drainage relative to water in the froth. Therefore, more particles overcome the downward gravitational force and are entrained to the concentrate. This is expected in the flotation operated at a relatively high air rate and shallow froth depth. However, when very low air rates and deep froths are used, multiple mechanisms will be responsible for the effect of air rate and froth depth on the entrainment factor. In addition to the abovementioned mechanism, the entrapment may account for the high values of the entrainment factor under these circumstances. Although it is difficult to distinguish entrapment from entrainment, this study provides experimental evidence how air rate and froth depth affect the entrainment factor outside of these conditions.

4. Conclusions

Air rate and froth depth were found to have a marked effect on entrainment factor. Both variables interacted to affect entrainment factor, and this interactive effect depended strongly on particle size. In general, the entrainment factor increased with the increasing air rate at relatively shallow froths. At relatively high air rates, the entrainment factor decreased as froth depth increased. At a very low air rate and deep froth, higher entrainment values were observed for mid-size and coarse particles.

Multiple mechanisms were responsible for the effect of air rate and froth depth on entrainment factor. At a relatively high air rate and shallow froth, entrainment factor had a linear correlation with the effective liquid velocity at the interface, suggesting that drag force dominated the change in the entrainment factor when air rate and froth depth were varied. At a very low air rate and deep froth, the entrainment factor for fine particles was also found to be strongly correlated with the effective liquid velocity at the interface, implying that the same mechanism applies. While for the high entrainment factor for mid-size and coarse particles under this condition, the entrapment of solid particles may be the primary determinant.

Acknowledgments

The funding provided by the Fundamental Research Funds for the Central Universities (No.2018QNA29) to support the work is greatly acknowledged. The first author would also like to thank Professor Kym Runge from the University of Queensland for the useful discussion on this topic.

References

AKTAS, Z., CILLIERS, J.J., BANFORD, A.W., 2008. *Dynamic froth stability: Particle size, airflow rate and conditioning time effects*. Int. J. Miner. Process. 87, 65-71.

ATA, S., AHMED, N., JAMESON, G.J., 2004. *The effect of hydrophobicity on the drainage of gangue minerals in flotation froths*. Miner. Eng. 17, 897-901.

BISSHOP, J.P., WHITE, M.E., 1976. *Study of particle entrainment in flotation froth*. Trans. Inst. Min. Metall. C85, 191-194.

CUTTING, G.W., WATSON, D., WHITEHEAD, A., BARBER, S.P., 1981. *Froth structure in continuous flotation cells: Relation to the prediction of plant performance from laboratory data using process models*. Int. J. Miner. Process. 7, 347-369.

ELGER, D.F., WILLIAMS, B.C., CROWE, C.T., ROBERSON, J.A. *Engineering Fluid Mechanics*. John Wiley & Sons, Inc, the USA.

ENGELBRECHT, J.A., WOODBURN, E.T., 1975. *The effect of froth height, aeration rate and gas precipitation on flotation*. J. South Afr. Inst. Min. Metall. 76, 125-132.

JOHNSON, N.W., 1972. *The flotation behaviour of some chalcopyrite ores.* PhD Thesis, The University of Queensland, Brisbane, Australia.

KRACHT, W., OROZCO, Y., ACUNA, C., 2016. *Effect of surfactant type on the entrainment factor and selectivity of flotation at laboratory scale.* Miner. Eng. 92, 216-220.

LANGBERG, D.E., JAMESON, G.J., 1989. *Factors affecting the water recovery rate during froth flotation*. Chemeca 89: Technology for Our Third Century; the Seventeenth Australasian Chemical Engineering Conference, Gold Coast, Australasian Chemical Engineering Conference, 295–301.

LYNCH, A.J., JOHNSON, N.W., MANLAPIG, E.V., THORNE, C., 1981. *Mineral and Coal Flotation Circuits*. Elsevier: Amsterdam.

MAACHAR, A., DOBBY, G.S., 1992. *Measurement of feed water recovery and entrainment solids recovery in flotation columns.* Can. Metall. Quart. 31, 167-172.

NEETHLING, S.J., CILLIERS, J.J., 2002a. *The entrainment of gangue into a flotation froth.* Int. J. Miner. Process. 64, 123-134.

NEETHLING, S.J., CILLIERS, J.J., 2002b. *Solid motion in foams*. Chem. Eng. Sci. 57, 607-615.

NEETHLING, S.J., CILLIERS, J.J., 2009. *The entrainment factor in froth flotation: Model for particle size and other operating parameter effects*. Int. J. Miner. Process. 93, 141-148.

NELSON, M.G., LELINSKI, D., 2000. *Hydrodynamic design of self-aerating flotation machines*. Miner. Eng. 13, 991-998.

NGUYEN, A.V., SCHULZE, H.J., 2004. *Colloidal Science of Flotation.* Marcel Dekker Inc.: New York.

ROSS, V.E, VAN DEVENTER, J.S.J., 1988. *Mass transport in flotation column froths*. Column Flotation'88: Proceedings of an International Symposium SME-AIME Annual Meeting, Phoenix, Arizona, 129-39.

SAVASSI, O.N., ALEXANDER, D.J., FRANZIDIS, J.P., MANLAPIG, E.V., 1998. *An empirical model for entrainment in industrial flotation plants*. Miner. Eng. 11, 243-256.

SMITH, P.G., WARREN, L.J., 1989. *Entrainment of particles into flotation froths.* Miner. Process. Extra. M. 5, 123-145.

SZATKOWSKI, M., 1987. *Factors influencing behaviour of flotation froth*. Inst. Min. Metall. Trans. Sect. C. Miner. Process. Extract. Metall. 96, 115-112.

WANG, L., 2017. *Entrainment of fine particles in froth flotation*. PhD thesis, The University of Queensland, Brisbane, Australia.

WANG, L., PENG, Y., RUNGE, K., 2016a. *Entrainment in froth flotation: The degree of entrainment and its contributing factors*. Powder Technol. 288, 202-211.

WANG, L., RUNGE, K., PENG, Y., VOS, C., 2016b. *An empirical model for the degree of entrainment in froth flotation based on particle size and density*. Miner. Eng. 98, 187-193.

WANG, L., RUNGE, K., PENG, Y., 2016c. *The observed effect of flotation operating conditions and particle properties on water recovery at laboratory scale*. Miner. Eng. 94, 83-93.

WANG, L., PENG, Y., RUNGE, K., 2017. *The mechanism responsible for the effect of frothers on the degree of entrainment in laboratory batch flotation*. Miner. Eng. 100, 124-131.

YIANATOS, J., BERGH, L., CONDORI, P., AGUILERA, J., 2001. *Hydrodynamic and metallurgical characterization of industrial flotation banks for control purposes*. Miner. Eng. 14, 1033-1046.

YIANATOS, J., CONTRERAS, F., 2010. *Particle entrainment model for industrial flotation cells*. Powder Technol. 197, 260-267.

ZHENG, X., FRANZIDIS, J.P., JOHNSON, N.W., MANLAPIG, E.V., 2005. *Modelling of entrainment in industrial flotation cells: The effect of solids suspension*. Miner. Eng. 18, 51-58.

ZHENG, X., FRANZIDIS, J.P., JOHNSON, N.W., 2006a. A*n evaluation of different models of water recovery in flotation*. Miner. Eng. 19, 871–882.

ZHENG, X., JOHNSON, N.W., FRANZIDIS, J.P., 2006b. *Modelling of entrainment in industrial flotation cells: Water recovery and degree of entrainment*. Miner. Eng. 19, 1191-1203.